*Asian Journal of Chemistry; Vol. 36, No. 10 (2024), 2385-2390*

ASIAN JOURNAL OF CHEMISTRY

https://doi.org/10.14233/ajchem.2024.32360

# Water Dispersible Poly(3,4-ethylenedioxythiophene) Nanogold Composites through Soft Template Route for Electrochemical Sensing of Ascorbic Acid

S. SIVAKALA[1,*], P.R. PAULCY RANI[2], ASHA S. KUMAR[3] and RESHMI JAYA RAVEENDRAN[1]

[1]Department of Chemistry, S.N. College, Chempazhanthy-695587, India
[2]Department of Chemistry, Government Womens College, Trivandrum-695014, India
[3]Department of Chemistry, S.N. College, Chathannoor-691579, India

*Corresponding author: E-mail: sivakalasnc@gmail.com

*Received*: 24 July 2024; *Accepted*: 7 September 2024; *Published online*: 30 September 2024; AJC-21769

This study presented the development of a water dispersible poly(3,4-ethylene dioxythiophene) (PEDOT) nanogold nanocomposite with a renewable resource-derived amphiphilic dopant, 3-pentadecylphenol-4-sulphonic acid (3-PDPSA). The amphiphilic dopant so designed is found to form stable emulsion with ethylenedioxythiopene (EDOT) with a wide composition range in water. The lyotropic behaviour of the PDPSA is found to be of complex nature at higher concentration higher than the micellar region. 3-PDPSA have built-in head-to-tail geometry effectively penetrates into PEDOT-Au chains to form highly organized nanowires. PEDOT-Au nanotubes are freely dispersible in water for various applications. PEDOT-Au is found to be an effective electrode modifier and acts as an electrochemical sensor for determining the concentration of ascorbic acid.

**Keywords: Polyethylene dioxythiophene, Electrochemical sensing, Antioxidants, Nanogold composite, Emulsion polymerization.**

## INTRODUCTION

When compared to single nanomaterials, multicomponent hybrids exhibit a more sensitive and quick current response due to their greater electrochemically active surface areas, which allow for the adsorption of target molecules [1]. Nanocomposite formation allows for the display of new or enhanced functional properties compared to those of the individual components. The nanoscale superparamagnetic properties of magnetite ($Fe_3O_4$) have made it useful in ferrofluids, MRI and magnetic separation [2-4]. Plasmon resonance, biocompatibility and surface-enhanced Raman spectroscopy (SERS) are three areas that could benefit from iron oxide nanoparticles that have been coated with metals like gold or silver [5-7]. Various methods have been used to create these nanocomposites, such as sputter coating in an ultrahigh vacuum (UHV) environment [8], deposition by high energy sources (like ultrasonication, γ-rays or high temperature treatment) [9-11] and the precipitation method.

Polyethylenedioxythiophene composite (PEDOT-Au) has importance especially in photovoltaics. The unique optical characteristics of coinage nanoparticles, particularly those of copper, silver and gold, have attracted a great deal of interest. Catalysis, photonics, photography, conductive inks, adhesives for various electronic components and thick film pastes are some of the many uses for silver and gold nanoparticles. It is possible to design the novel materials with inorganic and organic characteristic properties by choosing the inorganic and organic phases.

Relative to pure polyaniline, polyaniline composites containing noble metal nanoparticles exhibit superior electrical, catalytic and sensing properties [12]. Polyaniline silver nanocomposites have been synthesized using a variety of approaches. An *in situ* photo-redox approach was reported by Khanna *et al.* [13] for the synthesis of Ag/PANI nanocomposites. This process involved reducing silver salt in aniline using UV lamp radiation. In their study, Kang *et al.* [14] utilized γ-irradiation to create nanocomposites by oxidatively polymerizing silver colloids stabilized with polyaniline. Using *in situ* γ-radiation-induced chemical polymerization technique, core-shell silver nanocomposites were synthesized by Karim *et al.* [15], whereas Du *et al.* [16] reported the one-pot synthesis method of Ag/polyaniline nanoparticles. Pillalamarri *et al.* [17] also prepared composite materials with polyaniline nanofibers decorated with noble metal (Ag or Au) nanoparticles using γ-radiolysis. Using the unsymmetrical square wave current technology, Zhou *et al*. [18] produced the PANI silver nanocomposite film. In this method, an anodic process for aniline monomer polymerization was combined with a cathodic process for metal ionic electrodeposition.

Antioxidants are the chemical compounds that can terminate the radical-induced chain reactions. L-Ascorbic acid or Vitamin C, is a powerful antioxidant found in various food and beverages, serving as a chemical indicator for assessing food degradation and product quality. The estimation of ascorbic acid has garnered significant attention in biomedical engineering as well as in the food and pharmaceutical industries, due to its various functions [19]. Numerous analytical techniques, including titrimetry, spectrophotometry, fluorimetry and chromatography, were developed for its analysis [20]. These approaches often yield consistent findings with great sensitivity and excellent selectivity. All these analytical procedures require advanced instrumentation and chemical manipulation of samples prior to measurement, which can be time-consuming and impractical. Electrochemical analysis has advantages over other approaches, including simplicity, precision, reproducibility, specificity for diverse chemical species and adaptability to minimal sample volumes.

This study outlines a straightforward method for synthesizing PEDOT-Au nanocomposite fibers, which aims to examine the impact of gold nanoparticles on the electrical characteristics of PEDOT-Au, considering that incorporation of nanoparticles can improve the conductivity of the polymer matrix. The resultant composite was determined to be an effective electrode modification for the detection of ascorbic acid.

## EXPERIMENTAL

Highest grade of ethylenedioxy thiophene (EDOT), ferric chloride, ascorbic acid and auryl chloride were purchased from Sigma Aldrich, USA and used as such.

**Preparation of PEDOT-Au nanocomposite fibres:** A 0.1 M of EDOT prepared in water was added dropwise to a stirring solution containing 0.05 M of 25 mL solution of $AuCl_3$ and 5 mL of 3-PDPSA to form an emulsion. The solution was then cooled in an ice bath and then added 25 mL of 0.1 M $FeCl_3$ solution dropwise while stirring. After the complete addition, the solution was continuously stirred further for 6 h at same temperature. Finally, water was added to obtain composite as precipitate, filtered, washed several times with ethanol and dried.

The optical properties were studied by absorption spectra in the range 300-900 nm using UV-Vis spectrophotometer (Shimadzu model 2100). The X-ray diffraction measurements were carried out by Rigaku Miniflex X-ray diffractometer using nickel filtered Cu$K\alpha$ radiation. At 30 ºC, the electrical conductivity (sdc) of pressed pellets of uniform size was measured using the four-probe method (Scientific Equipment, Roorkee, India). The conductivity ($\sigma_0$) was calculated using van der Pauw relation:

$$\sigma_0 = \left(\ln\frac{2}{\pi}d\right)\left(\frac{I}{V}\right)$$

where d is the thickness of film.

The samples were prepared by drop casting solution of gel ($2 \times 10^{-6}$ M) onto a carbon coated copper grid. The morphology was observed under transmission electron microscope (TEM) measurements (JEOL JEM1011) with an accelerating voltage of 80 kV. TEM images were obtained without staining and the FT-IR analysis were conducted with Nicolet impact 400D FT-IR spectrophotometer. The thermal stability analysis were performed at 20 ºC in nitrogen atmosphere using Schimadzu, DTG-60 differential thermogravimetry equipment. The performance and characteristics of the electrode was studied with respect to the surface concentration of PEDOT-Au at the electrode, response time, sensitivity, detection limit and storage life. Common potential interferents within the sample matrices were also evaluated to confirm the selection of the electrode.

## RESULTS AND DISCUSSION

A water dispersible poly(3,4-ethylene dioxythiophene) (PEDOT) nanogold composite was prepared through chemical oxidative polymerization of ethylenedioxythiopene (EDOT) in presence of 3-pentadecylphenol-4-sulphonic acid (3-PDPSA) as amphiphilic dopant as well as structure directing agent and $FeCl_3$ as oxidizing agent. Here, the PEDOT-Au composite's size and form are controlled by the structure-directing agent, which is the self-assembling micelles of dopant/surfactant. The PEDOT-Au composite was characterized by FTIR, UV-visible spectro-scopy, XRD, TGA and TEM.

**FTIR spectral studies:** FTIR spectra of the pure PEDOT as well PEDOT-Au nanocomposite are shown in Fig. 1. The FT-IR spectra revealed that PEDOT-Au exhibited the quinoidal C-C and C-C structures, which are attributed for the thiophene ring vibration at 1460 $cm^{-1}$ and 1380 $cm^{-1}$, respectively. Moreover, the C-O-C bond stretching was attributed to the vibrations at 1170 and 1000 $cm^{-1}$, while, the C-S bond vibrations in the thiophene ring were appeared at 974 and 850 $cm^{-1}$ [12]. The

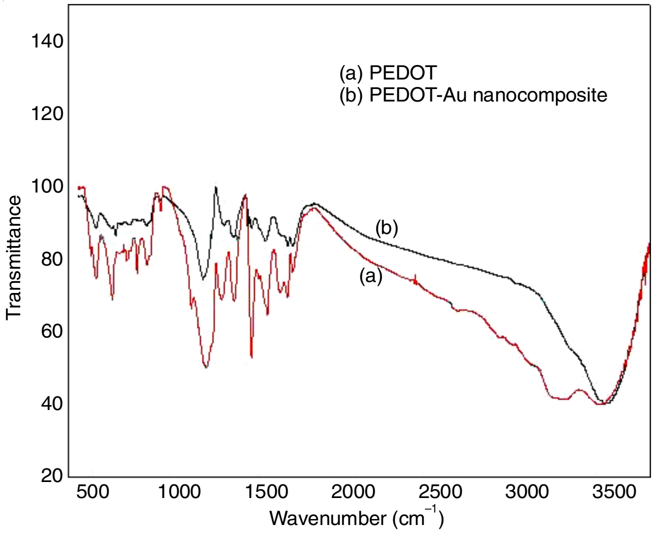

Fig. 1. FTIR spectra of PEDOT and PEDOT Au composite

shifts in the peak locations corresponding to quinoid ring C-O-C stretching and thiophene ring C-H bending happened. The conduction mechanism in PANI/gold nanocomposites proposed by Tseng *et al.* [21] is supported by these results. In addition, the nanocomposite has lower band intensities because of the Au nanoparticles in the polymer matrix, which is consistent with the observation of Khanna *et al.* [13].

**UV-Vis spectral studies:** The UV-Vis spectral approach is a highly sensitive method for examining the characteristics of prolongation in conducting polymers, clearly distinguishing between the conducting and non-conducting states of the molecule. It exhibited two maxima around 330-430 nm and a free carrier peak from 700 nm to 900 nm. The initial maxima can be assigned due to the $\pi$-$\pi$* electronic transition and the second maxima arising from the cationic radical ion (polaron band) of the doped PEDOT-Au. This free carrier peak from 700 nm confirms the high conducting nature of doped PEDOT-Au.

**Thermal studies:** Fig. 2 displays the thermogram of the PEDOT-Au nanocomposite. Up to 100 ºC, the initial loss of mass is caused by evaporization of water, whereas surfactant evaporation occurs between 140 and 435 ºC. A remarkable weight loss occurs after 435 ºC, which results in the breakdown in the polymer's structure. Since the structural disintegration in the nanocomposite begins above 470 ºC, one can inferred that the polymer's thermal stability is enhanced by the nanofiller layer of gold. The present observation is consistent with the findings of Khanna *et al.* [13], who also reported that the composite decomposes at a higher temperature when loaded with gold nanoparticles compared to the polymer alone.

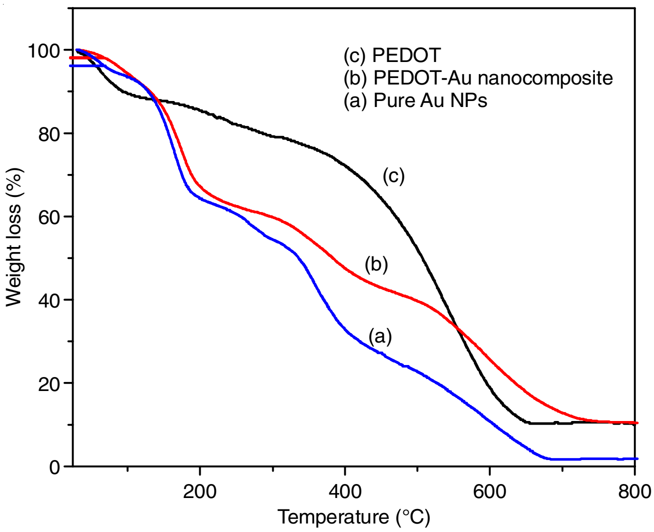

Fig. 2. Thermograms of pure Au NPs, PEDOT and PEDOT-Au nanocomposite

**X-ray diffraction studies:** Fig. 3 shows the XRD patterns of pure Au nanoparticles, 0.25% Au and PEDOT-Au nanocomposite. All peaks in the XRD patterns are in agreement with the literature values of gold nanoparticles. No other peak than Au was observed, which confirms that polymer has only Au nanoparticles incorporated in the polymer matrix.

**Morphological studies:** Fig. 4 shows the SEM and TEM images of the PEDOT-Au nanocomposite. The formation of nanocomposite may be resulting from self assembly of monomer PDPSA complex. The monomer and the dopant form surfactant micelle adduct and will self-assemble to form supramolecular assembly arising from various non-covalent interactions like electrostatic layer by layer assembling, $\pi$–$\pi$ interaction, hydrogen bonding, *etc*. The dark portion represent the Au nanoparticles entrapped inside the nano fibres of PEDOT.

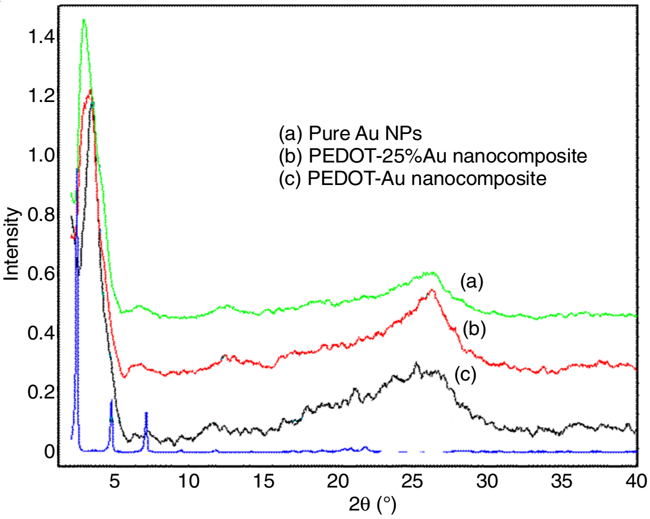

Fig. 3. X-ray diffractograms of PEDOT and PEDOT-Au composite

**Electrical conductivity studies:** The electrical conductivity of the nanocomposite was observed to be in the range of 0.1-1 S/cm$^{-1}$.

**PEDOT-Au as electrochemical sensor for ascorbic acid:** The electrically nanostructured PEDOT-Au was used as an Pt electrode modifier for the analysis of ascorbic acid. The cyclic voltammogram of PEDOT-Au was recorded in the potential range of –1 to 1 V starting and is displayed in Fig. 5. It exhibited a sharp oxidation peak at - 0.7334 V, which corresponds to the oxidation of PEDOT. The sharpness of the peak reveals its high rate of electron transfer in the oxidation process. Another medium peak observed at 0.0066 V corresponds to the reduction of PEDOT. The less intensity of the peak reveals its slow rate of electron transfer in the reduction process. The addition of ascorbic acid varies the current intensity at this peak and this variation can be related to the concentration of ascorbic acid.

**Estimation of ascorbic acid:** At a high over potential of 0.5 V, there is a broad peak which indicates the irreversible oxidation of ascorbic acid at the bare electrode. Electrode fouling by ascorbic acid oxidation products at the bare electrode likely causes the slow electron transfer kinetics, which in turn causes the electrode response to be non-reproducible. Real analyte solutions, however, often contain a plenty of oxidizable species that can also be oxidized anodically at a relatively high electrode potential. Thus, these substances can exceed anodic current response corresponding to electro-oxidation of ascorbic acid. So, it is of considerably great importance to create electrocatalytically active electrode surface that could enable to lower the electro-oxidation potential of ascorbate up to an appropriate level. The Pt/PEDOT -Au electrode could detect ascorbic acid at a lower potential of 0.1097 V with a increase in the reduction current intensity. The negative shift of oxidation potential with

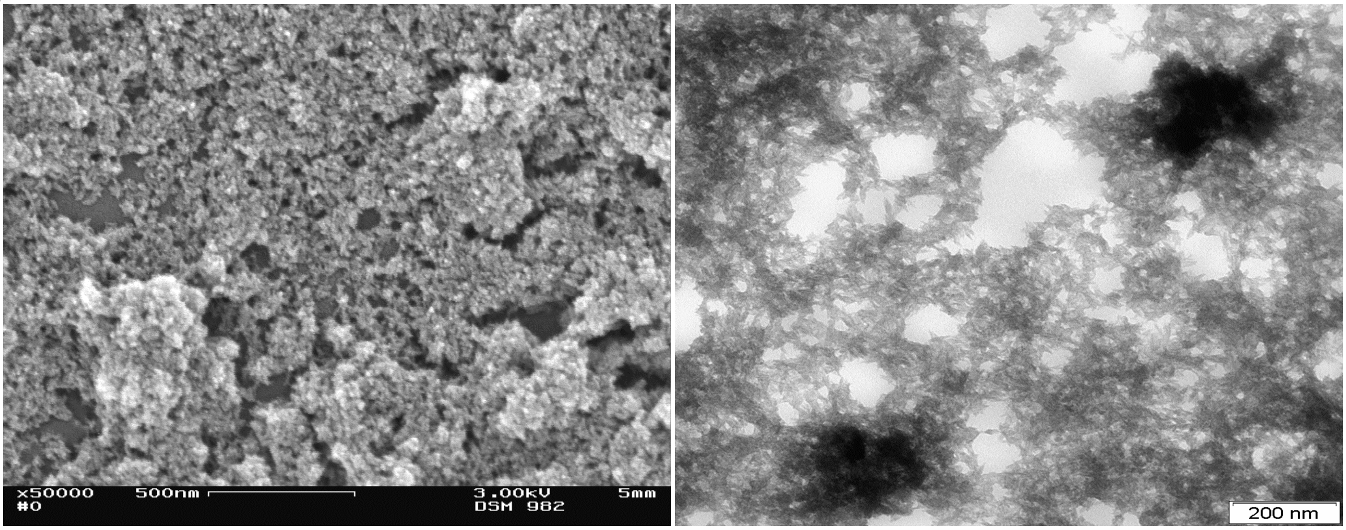

Fig. 4. SEM and TEM images of the composite

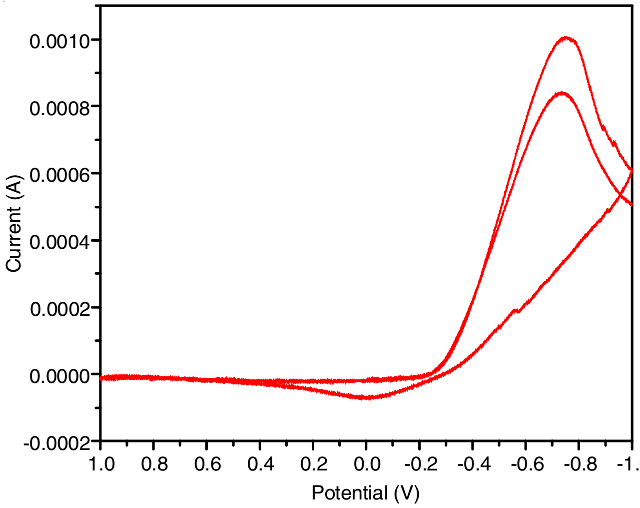

Fig. 5. Typical CV diagram of PEDOT-Au/pt electrode

increase in the oxidation current of ascorbic acid may be due to the favourable electrostatic attraction between the cationic PEDOT and anionic ascorbic acid. Such an interaction would lead to the increase in the reactivity of ascorbic acid within the electrode. The significant variation in the voltammetric response of ascorbic acid with PEDOT-Au/Pt electrode confirms the sensitivity of ascorbic acid. Typical CV diagram of PEDOT-Au/Pt electrode modifier after the addition of ascorbic acid is shown in Fig. 6.

On adding ascorbic acid into the PEDOT-Au solution, the cathodic current at potential of 0.1097V increased. The experiments were performed with increasing concentration of ascorbic acid from 100-1000 µL (1 µM) and the corresponding cyclic voltammograms are shown in Fig. 7. Linearity of the amperometric response of ascorbic acid was checked by plotting current against concentration and is shown in Fig. 8, which observed as a straight line with a correlation coefficient of 0.998. The enhancement in the amperometric response observed at higher concentration of ascorbic acid is due to the diffusion of radicals to PEDOT solution, which maintains in the electronic interaction with the Pt electrode surface.

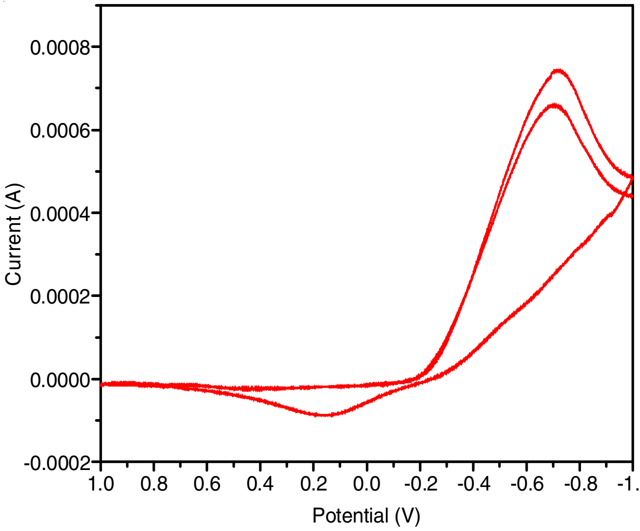

Fig. 6. Typical CV diagram of PEDOT-Au/pt electrode after the addition of ascorbic acid

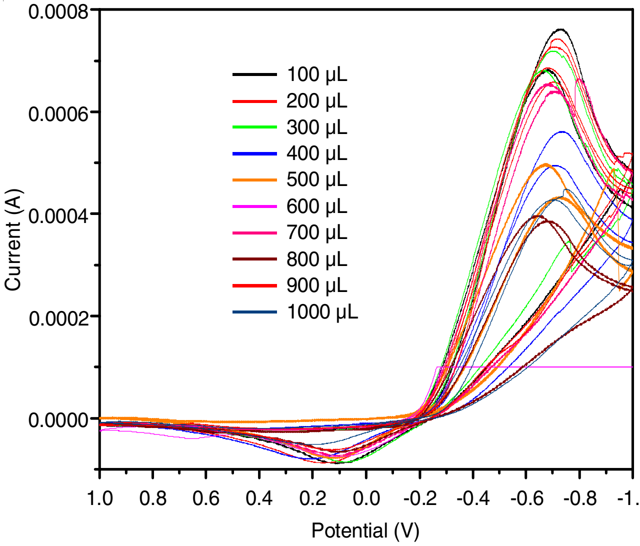

Fig. 7. Overlayed cyclic voltammograms of ascorbic acid at different concentrations

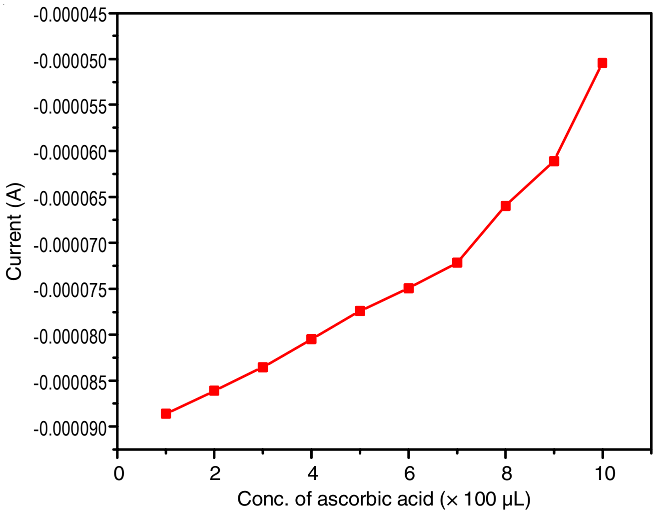

Fig. 8. Linearity of the amperometric response of CV at varying concentration of ascorbic acid

**Sensitivity studies:** The sensitivity of the electrode was assessed by introducing a known quantity of ascorbic acid and subsequently back-calculating its concentration from the linear curve. Sensitivity was observed with a minimum relative standard deviation of 1-2 % (Fig. 9). Such sensitivity may be ascribed due to the huge surface area, which would load more ascorbic acid and would be advantageous to the transfer of the electron to the electrode. Response time was observed to be less than 15 s to reach steady-state, proving the high catalytic efficiency of PEDOT-Au nanocomposite. In general, the PEDOT-Au nanocomposite transduces as well as amplifies the signal and increases the electrode's sensitivity to ascorbic acid assay.

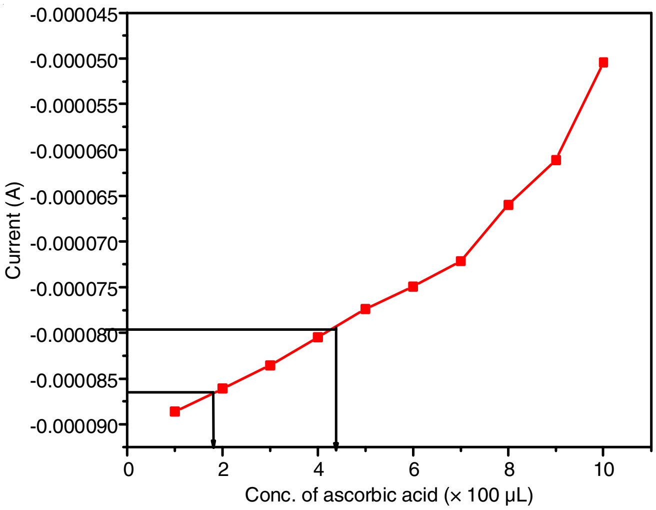

Fig. 9. Checking the sensitivity of the PEDOT-Au/pt based amperometric sensor for ascorbic acid

**Storage stability:** Fig. 10 shows that the electroactive species remains active and maintains its activity even after 3 weeks, since the electrode current remained stable over the 50 cycles of continuous scanning between 1 V and -1 V. Additionally, no emission was observed when this modified electrode was swept in an ascorbic acid solution for an extended period of time. Since it is stable and easy to fabricate, it holds great promise for the future of these sensors. The reproducibility of the results was also evaluated by repeating the process at different time intervals over a month and comparing the intensity of the oxidation peak with that of the initial stage. At 0.1097 V, the ascorbic acid oxidation occurred in almost all the experiments with the smallest reduction in background current, which shows that the PEDOT-Au modified Pt electrode sensor is suitable for ascorbic acid assay.

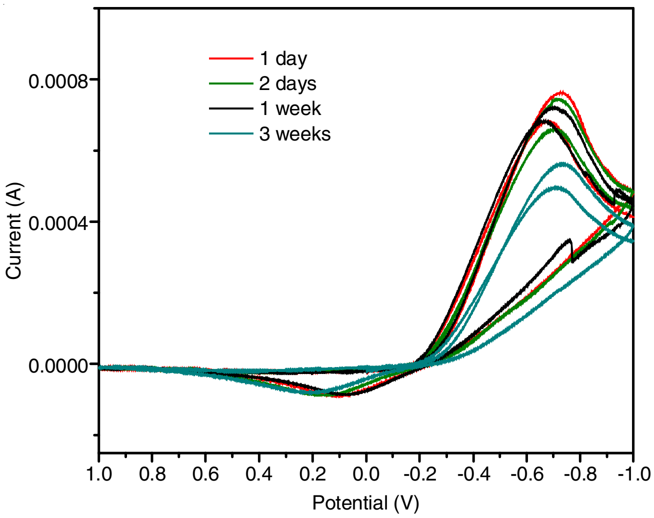

Fig. 10. Studies on the storage stability of PEDOT-Au/Pt electrode

**Effect of interference on the determination of ascorbic acid:** To evaluate the selectivity of PEDOT-Au/Pt sensor, the effect of common potentially interfering compounds (organic acids, antioxidants and sugars) were investigated and is shown in Fig. 11. Concentration higher than those of the natural levels expected in the food samples were tested by measuring the ascorbic acid content of 1 mM stock solution in presence of the potential interferents like glucose, tartaric acid, phenol and citric acid.

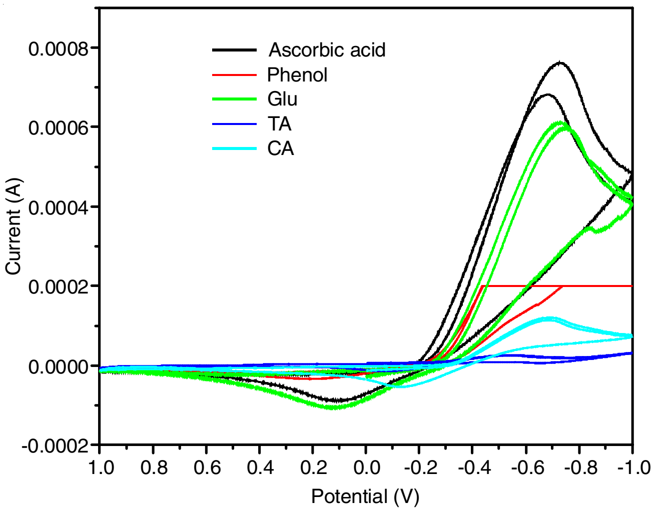

Fig. 11. Interference studies

**Detection limit:** The detection limit of the PEDOT-Au/Pt modified electrode for the analysis of ascorbic acid was determined by measuring the oxidation potential current using different molar concentration of ascorbic acid and the typical overlayed diagrams are shown in Fig. 12. It exhibited deviation in the potential at the nanomolar level revealing the detection limit of nanomolar concentration.

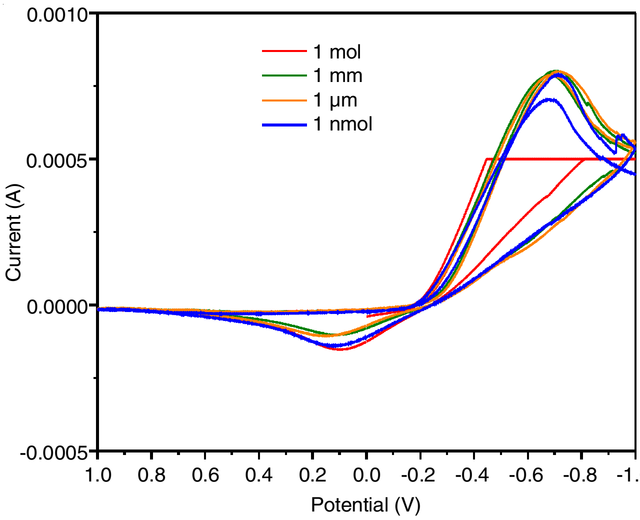

Fig. 12. Overlayed CV diagram at different concentration of ascorbic acid showing detection limit in nM concentration of ascorbic acid

## Conclusion

Water dispersible poly(3,4-ethylenedioxythiophene) nanogold (PEDOT-Au) composite could be prepared by employing low cost renewable resource based amphiphilic molecule 3-pentadecyl-phenol-4-sulphonic acid as surfactant as well as dopant in extremely low concentration. Studies showed that surfactant forms self assembled micelles in the medium, which act as soft template and act as a structure-directing agent for the formation of these nanotubes, nanowires in the present as a soft template. According to the results obtained from the SEM, XRD and TEM, the nanocomposite exhibited the formation of micro/nano structured spherical aggregates. The absorbance spectra of the PEDOT-Au indicated the formation of free carrier tail due to presence of polar band. The shape, size and electronic structure of the formed nanostructured PEDOT-Au depends on structure of the amphiphilic molecule, amount of the surfactant, reaction medium and temperature of the reaction. Thus, the PEDOT-Au is found to be an effective modifier and as an electrochemical sensor for determining the concentration of antioxidants in solutions and mixtures.

## ACKNOWLEDGEMENTS

The authors are grateful to Director, NIIST, Trivandrum, India for the charecterization facilities.

## CONFLICT OF INTEREST

The authors declare that there is no conflict of interests regarding the publication of this article.

## REFERENCES

1. A.G. Díez, M. Rincón-Iglesias, S. Lanceros-Méndez, J. Reguera and E. Lizundia, *Mater. Today Chem.*, **26**, 101220 (2022); https://doi.org/10.1016/j.mtchem.2022.101220
2. B. Belaabed, J.L. Wojkiewicz, S. Lamouri, N. El Kamchi and T. Lasri, *J. Alloys Compd.*, **527**, 137 (2012); https://doi.org/10.1016/j.jallcom.2012.02.179
3. P. Calvo-Marzal, S.S. Rosatto, P.A. Granjeiro, H. Aoyama and L.T. Kubota, *Anal. Chim. Acta*, **441**, 207 (2001); https://doi.org/10.1016/S0003-2670(01)01120-5
4. R.S. Nicholson and I. Shain, *Anal. Chem.*, **37**, 190 (1965); https://doi.org/10.1021/ac60221a003
5. X. Zhang, Z. Liu, J. Zhang and C. Robinson, *Chem. Commun.*, **16**, 1852 (2004); https://doi.org/10.1039/b405255b
6. G.B. Street, S.E. Lindsey, A.I. Nazzal and K.J. Wynne, *Mol. Crys. Liq. Cryst.*, **118**, 137 (1985); https://doi.org/10.1080/00268948508076201
7. Y. Lu, Y. Mei, M. Schrinner, M. Ballauff, M.W. Möller and J. Breu, *J. Phys. Chem. C*, **111**, 7676 (2007); https://doi.org/10.1021/jp070973m
8. E. Song and J.W. Choi, *Nanomaterials*, **3**, 498 (2013); https://doi.org/10.3390/nano3030498
9. M. Zaarour, M. El Roz, B. Dong, R. Retoux, R. Aad, J. Cardin, C. Dufour, F. Gourbilleau, J.-P. Gilson and S. Mintova, *Langmuir*, **30**, 6250 (2014); https://doi.org/10.1021/la5006743
10. Q. Guo, R. Ghadiri, T. Weigel, A. Aumann, E. Gurevich, C. Esen, O. Medenbach, W. Cheng, B. Chichkov and A. Ostendorf, *Polymers*, **6**, 2037 (2014); https://doi.org/10.3390/polym6072037
11. S. Wang, Y. Kang, I. Wang, H. Zhang, Y. Wang and Y. Wang, *Sens. Actuators B Chem.*, **182**, 467 (2013); https://doi.org/10.1016/j.snb.2013.03.042
12. M. El Rhazi, S. Majid, M. Elbasri, F.E. Salih, L. Oularbi and K. Lafdi, *Int. Nano Lett.*, **8**, 79 (2018); https://doi.org/10.1007/s40089-018-0238-2
13. P.K. Khanna, N. Singh, S. Charan, A.K. Viswanath, *Mater. Chem. Phys.*, **92**, 214 (2005); https://doi.org/10.1016/j.matchemphys.2005.01.011
14. Y.O. Kang, S.H. Choi, A. Gopalan, K.P. Lee, H.D. Kang HD and Y.S. Song, *J. Non-Cryst. Solids*, **352**, 463 (2006); https://doi.org/10.1016/j.jnoncrysol.2006.01.043
15. M.R. Karim, K.T. Lim, C.J. Lee, M.T.I. Bhuiyan, H.J. Kim, L.S. Park and M.S. Lee, *J. Polym. Sci.: Part A Polym. Chem.*, **45**, 5741 (2007); https://doi.org/10.1002/pola.22323
16. J.M. Du, Z.M. Liu, B.X. Han, Z.H. Li, J.L. Zhang and Y. Huang, *Micropor. Macropor. Mater.*, **84**, 254 (2005); https://doi.org/10.1016/j.micromeso.2005.05.036
17. S.K. Pillalamarri, F D. Blum, A.T. Tokuhiro, J.G. Story and M.F. Bertino, *Chem. Mater.*, **17**, 5941 (2005); https://doi.org/10.1021/cm0488478
18. H.H. Zhou, X.H. Ning, S.L. Li, J.H. Chen and Y.F. Kuang, *Thin Solid Films*, **510**, 164 (2006); https://doi.org/10.1016/j.tsf.2005.12.310
19. M. Dosedel, E. Jirkovský, K. Macáková, L.K. Krcmová, L. Javorská, J. Pourová, L. Mercolini, F. Remião, L. Nováková and P. Mladenka, *Nutrients*, **13**, 615 (2021); https://doi.org/10.3390/nu13020615
20. A. Husain, S. Parveen, M. Umar, H.P. Jethani, Abubakar and S. Kaushal, *J. Pharm. Med. Chem.*, **6**, 69 (2020); https://doi.org/10.21088/jpmc.2395.6615.6220.7
21. R.J. Tseng, J. Huang, J. Ouyang, R.B. Kaner and Y. Yang, *Nano Lett.*, **5**, 1077 (2005); https://doi.org/10.1021/nl050587l